*Impact Factor (SJIF): 3.632*

**International Journal of Advance Research in Engineering, Science & Technology**

*e-ISSN: 2393-9877, p-ISSN: 2394-2444*
***Volume 3, Issue 4, April -2016***

# Comparative analysis of the Combustion in Gas Turbine Can-Type Combustion Chamber

**Firoj H. Pathan[1], Dinesh K. Dabhi[2], Nikul K. Patel[3]**
[1] *Mechanical Department, Vadodara Institute of Engineering, Vadodara, India*
*Email: firojpathan_07@yahoo.com*
[2] *Mechanical Department, Vadodara Institute of Engineering, Vadodara, India*
*Email: dineshdabhi79@gmail.com*
[3] *Mechanical Department, The M S University of Baroda, Vadodara, India*
*Email: nikulatmsu@gmail.com*

***Abstract — Comparative analysis of the combustion of methane air mixture in gas turbine Can- combustion chamber is presented in this study. The analysis is done on CFD software with CFX solver. The motive of this study is to understand the combustion phenomena and resulted emissions. With the high cycle temperature of modern gas turbine, mechanical design remains difficult and a mechanical development program is inevitable. The rapidly increasing use of Computational Fluid Dynamics (CFD) in recent years has had a major impact on the design process, greatly increasing the understanding of the complex flow and so reducing the amount of trial and error required. The gas turbine Can-combustion chamber is designed to burn the fuel efficiently, reduce the emissions, and lower the wall temperature. In this study the mathematical models used for combustion consist of the PDF Flame let Model and Eddy Dissipation Combustion Model for non premixed gas combustion. The outcome of the work will help in finding out the predictions of PDF Flame let Model and Eddy Dissipation Combustion Model for non premixed gas combustion with geometry of the combustion chamber which will lead to less emission.***

***Keywords— PDF Flame let Model, Eddy Dissipation Combustion Model, Combustion, CFD***

## I. INTRODUCTION

THE design of a gas turbine combustion system is a complex process involving fluid dynamics, combustion and mechanical design. For many years the combustion system was much less amenable to theoretical treatment than other components of the gas turbine and development program required a considerable amount of trial and error. With the high cycle temperature of modern gas turbine, mechanical design remains difficult and a mechanical development program is inevitable [1]. Kuijk et. al. [2] optimized the design for biomass combustion furnaces for NOx-emission reduction. In this study, the Eddy Dissipation Concept and the PDF-flamelet approach compared with the experimental results. They found these two models are quite close, but deviate significantly from the measurements quantitatively. Chaouki Ghenai [3] performed a numerical investigation of the combustion of syngas fuel mixture in gas turbine can combustor to understand the impact of the variability in the alternative fuel composition and heating value on combustion performance and emissions. The composition of the fuel burned in can combustor was changed from natural gas (methane) to syngas fuel with hydrogen to carbon monoxide ($H_2$/CO) volume ratio ranging from 0.63 to 2.36. Results show the changes in gas turbine can combustor performance with the same power generation when natural gas or methane fuel is replace by syngas fuels. The gas temperature for the all five syngas shows a lower gas temperature compared to the temperature of methane. The gas temperature reduction depends on lower heating value and the combustible and non-combustible constituents in the syngas fuel which results in to less emission. Furuhata et. al. [4] carried out experiment on low $NO_x$ combustor for kerosene-fueled micro gas turbine based on a new concept was proposed and the combustion characteristics of the prototype combustor were investigated. The new concept combustor consisted of primary and secondary combustion zones, and they were connected by a throat. A swirler was set between the primary and secondary combustion zones. In order to enhance the recirculation of burned gas in the primary combustion zone, the combustion air was introduced through the swirler and forced to flow upward to the combustor bottom, from where fuel spray was supplied through a nozzle. An optimum configuration of the primary combustion zone such as length of primary zone, swirler vane angle, diameter of throat, etc. were investigated to achieve high combustion stability and low emission in wide ranges of fuel flow rate and excess air ratio. Krishna and Ganesan [5] carried

out CFD analysis of flow through vane swirlers. The present work reports a computational study of steady flow through vane swirlers for various vane angles from 15° to 60° in steps of 15°. Flow has been simulated by solving the appropriate governing equations, namely, conservation of mass and momentum using the SIMPLE-algorithm. Turbulence has been modeled using Reynolds's Stress Model (RSM). They found that the RSM seems to be appropriate for swirling flows, especially for flows with high swirl, as in the case of gas turbine combustors. In this study various parameters like air-fuel ratio, swirler angle of primary air inlet are changed to investigate the effect of these parameters on combustion chamber performance and emissions. In this study the mathematical models used for combustion consist of the k-ε model for turbulent flow, PDF flame let model and eddy dissipation combustion models for non premixed gas combustion, and P-1 radiation model. Comparison of the PDF flame let and eddy dissipation combustion model for non premixed gas combustion is presented in this study.

## II. MODELING, MESHING AND BOUNDARY CONDITIONS

### 2.1. PDF Flame let Model

The mathematical equations describing the fuel combustion are based on the equations of conservation of mass, momentum, and energy together with other supplementary equations for the turbulence and combustion. The standard k-ε turbulence model is used in this study. The equations for the turbulent kinetic energy k and the dissipation rate of the turbulent kinetic energy ε are solved. For non premixed combustion modeling, the mixture fraction/PDF model is used. In non-premixed combustion, fuel and oxidizer enter the reaction zone in distinct streams. The PDF/mixture fraction model is used for non premixed combustion modeling. In this approach individual species transport equations are not solved. Instead, equation for the conserved scalar (f) is solved, and individual component concentrations are derived from the predicted mixture fraction distribution. The P-1 radiation model is used in this study to simulate the radiation from the flame.

### 2.2. Eddy Dissipation Combustion Model

In this study Eddy Dissipation Combustion Model is also used to understand the combustion process and comparison with the PDF flame let combustion model. The eddy dissipation model is based on the concept that chemical reaction is fast relative to transport processes in the flow. When reactants mix at the molecular level, they instantaneously form products. The model assumes that the reaction rate may be related directly to the time required to mix reactants at the molecular level. In turbulent flows, this mixing time is dominated by the eddy properties, and therefore, the rate is proportional to a mixing time defined by the turbulent kinetic energy, k and dissipation, $\varepsilon$. This concept of reaction control is applicable in many industrial combustion problems where reaction rates are fast compared to reactant mixing rates.

### 2.3. Geometry

The basic geometry of the gas turbine can combustor is shown in Fig. 1. The size of the combustor is 590mm in the Z direction, 220mm in the Y direction, and 250mm in the X direction. The primary inlet air is guided by vanes to give the air a swirling velocity component. The injection diameter of primary air injector diameter is 100 mm. The fuel is injected through six fuel inlets in the swirling primary air flow. The fuel injector diameter is 4.2 mm for one hole. The secondary air is injected in the combustion chamber through six side air inlets each with an area of 33.50 $mm^2$. The can combustor outlet has a rectangular shape with an area of 0.0150 $m^2$. The dimensions of this geometry are taken from the Chauki Ghenai [3].

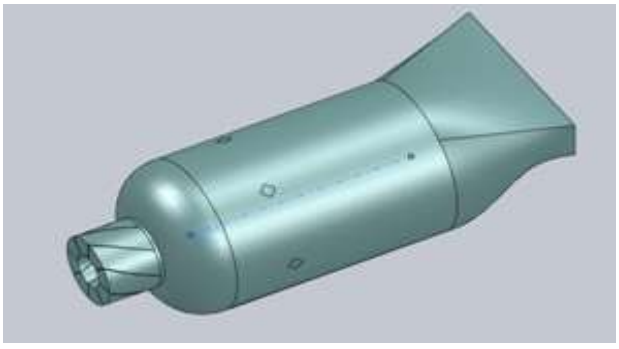

***Fig. 1. Basic Geometry of Can-Type Combustion Chamber***

### 2.4. Meshing

For the analysis of the combustion chamber, the commercial code CFX has been used in order to predict the centerline and

the wall temperature distribution as well as combustion phenomena. Mesh generation is very important part of the work that has to be done before starting any CFD calculations. For this investigation, the grid generation has been done on Workbench – Mesh (ICEM CFD). The mesh is generated by automatic method is used for meshing then generate the mesh. The mesh consist of 1, 80,002 elements or cells and 34724 nodes and element type is tetrahedral.

### 2.5. Boundary Conditions in CFX Pre

The different boundary conditions applied for flow analysis of gas turbine can-type combustion chamber are taken from the Ghenai [3]. The boundary conditions of the primary air are: The injection velocity is 10 m/s, the temperature is 300 K, the turbulence intensity is 10%, mixture fraction f = 0. The boundary conditions of the fuel are: Mass flow rate, 0.001 Kg/s, the temperature is 300 K, the turbulence intensity is 10%, mixture fraction f = 1. The boundary conditions of the secondary air are : The injection velocity is 6 m/s, the temperature is 300 K, the turbulence intensity is 10%, mixture fraction f = 0 and the secondary air is injected in the combustion chamber through six side air inlets. The boundary condition of the outlet of combustion is defined by providing pressure value. The relative pressure is taken zero Pascal. The finite volume method and the first-order upwind method are used to solve the governing equations. The convergence criteria are set to 10-6 for the continuity, momentum, and turbulent kinetic energy, dissipation rate of the turbulent kinetic energy, energy and the radiation equations and the mixture fraction.

## III. RESULTS AND DISCUSSION

### 3.1. Variation in velocity, temperature, NO mass fraction and CO mass fraction at different swirler angle

Fig.2 (a),(b),(c),(d),(e) show the axial velocity w (z-direction) profiles in radial distance for different axial location Z = 105 mm, Z=135 mm, Z=170 mm, Z=205 mm and Z=235 mm respectively. From Fig.2 (a), we can say that from outer (b) shows that at outer radius there is lowest velocity as movement towards the centerline this velocity increase. After achieving highest velocity, further it decreases at centerline. Here also the nature of graph is same as in Fig. 2 (a), but the decrease in velocity at centerline is less than the previous station z=105 mm. In this chart it is obvious that the as swirler

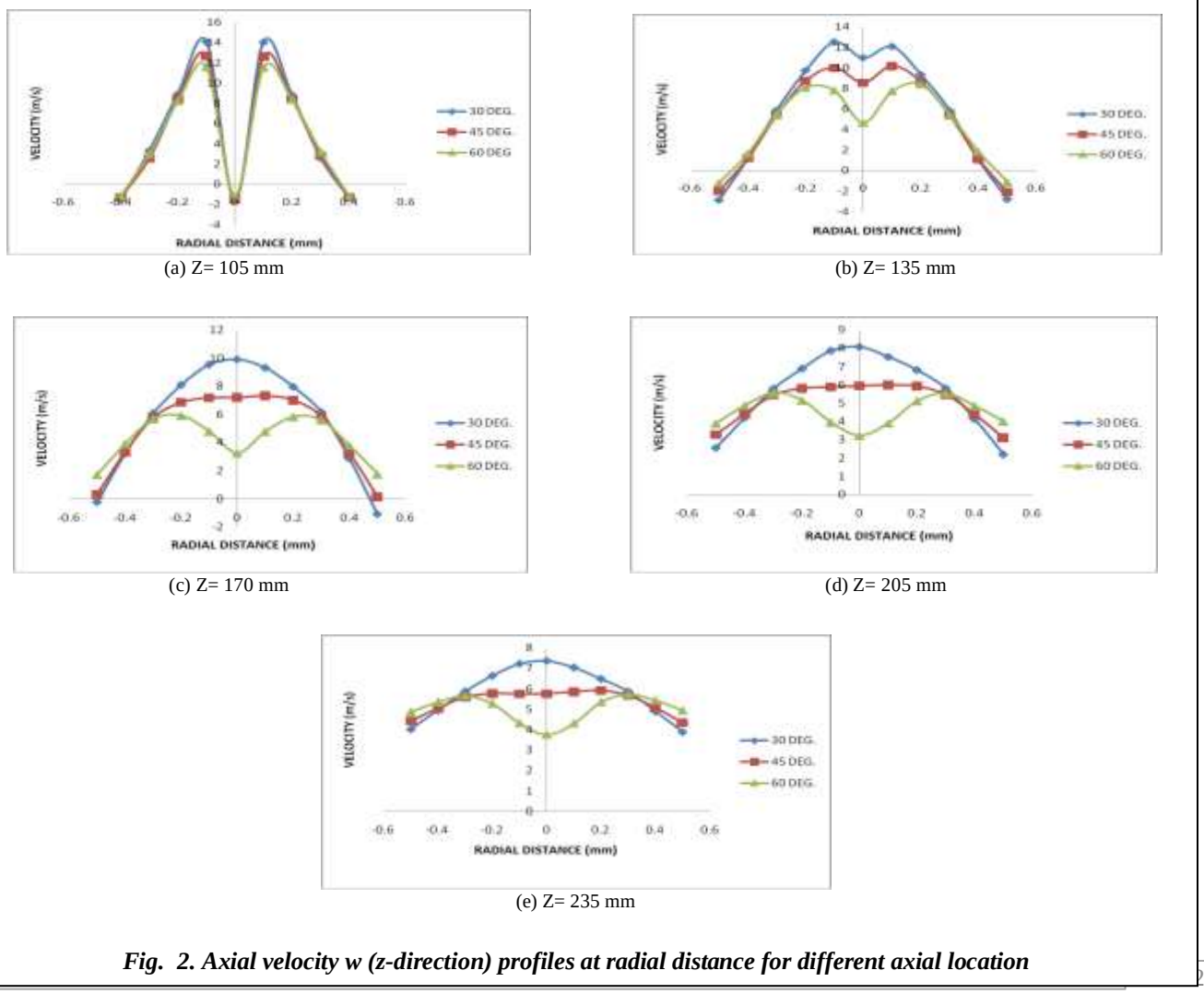


(a) Z= 105 mm

(b) Z= 135 mm

(c) Z= 170 mm

(d) Z= 205 mm

(e) Z= 235 mm

***Fig. 2. Axial velocity w (z-direction) profiles at radial distance for different axial location***

angle increases the core region velocity decreases, which provides the more residence time for greater mixing of flow for good combustion. For $30^0$ and $45^0$ , the center region velocity is high compare to the combustor wall velocity. So there will be no advantage of more residence time. For $60^0$, this velocity is less at center region, which provide more residence time for mixture for good combustion. One another thing is also observed from Fig. 2, that as further movement in axial direction the curves try to become flatter.Fig.3 shows the profile of temperature along center line. From this chart it is observed that the exit temperature achieved for 30° swirler is maximum compared to the 45° and 60°. At 60° lowest exits temperature is achieved. The NO emission is directly concerned with the temperature. The more the exit temperature more will be the NO emission. So the case of 60° swirler angle geometry of combustion chamber is best compared to the other swirler angle cases. Fig.4 depicts the profile of NO mass fraction along center line of the combustion chamber. From this profile it is observed that in 60° the lowest NO is found. From this we can conclude that NO is directly concerned with the temperature. It is thus important to reduce the temperature of gases coming out of the combustion chamber. This is achieved by mixing of air is sufficient quantity at secondary air inlet in combustion chamber.

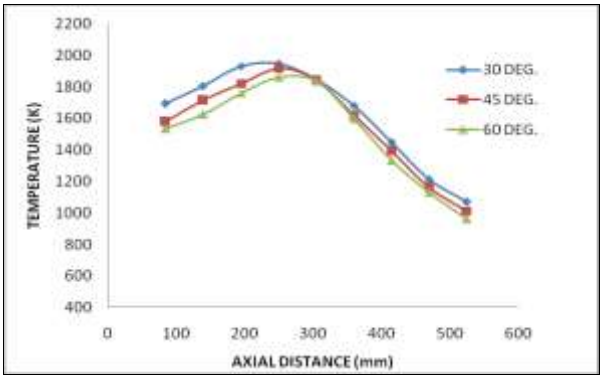


***Fig. 3. Profile of Temperature along the centre line of Can-Type Combustor Chamber***

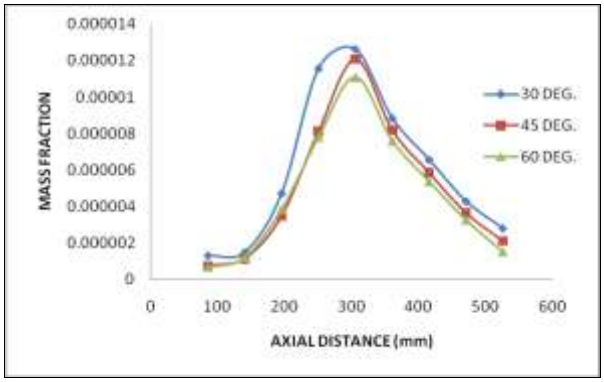


***Fig. 4. Profile of NO mass fraction along the centre line of Can-Type Combustor Chamber***

Fig. 5 shows the profile of $CO_2$ mass fraction along center line of the combustion chamber. It is observed from the profile that less mass fraction of $CO_2$ is achieved at 60° swirler geometry. In the case of 30° and 45° swirler the exit mass fraction of $CO_2$ are nearly same.

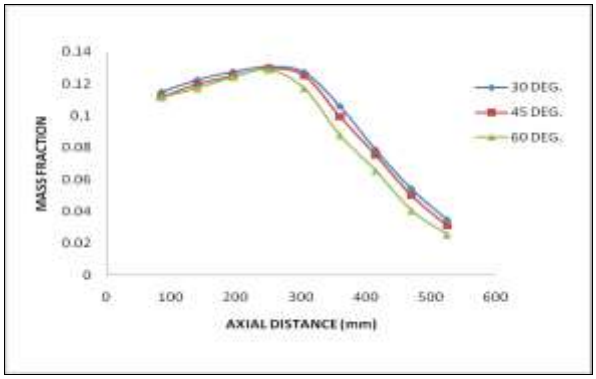


***Fig. 5. Profile of CO2 mass fraction along the centre line of Can-Type Combustor Chamber***

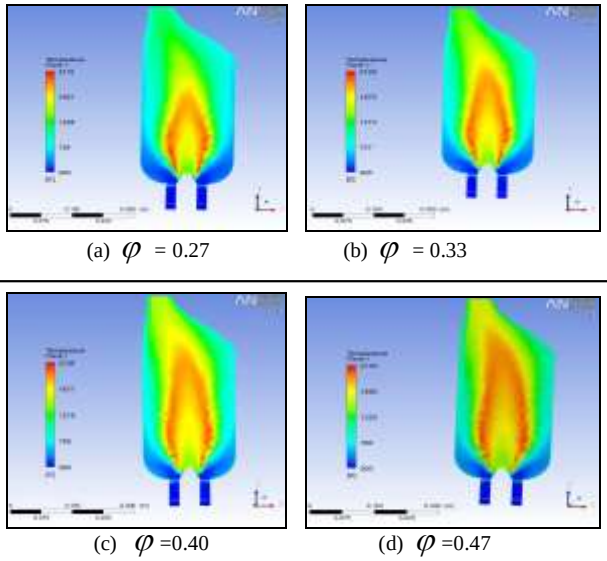

(a) $\varphi$ = 0.27 (b) $\varphi$ = 0.33

(c) $\varphi$ =0.40 (d) $\varphi$ =0.47

***Fig. 6. Contour of temperature at different equivalence ratio***

### 3.2. Parametric study

The Profile of Temperature along the centre line for the combustion of methane in gas turbine can-combustor is shown in Fig.3. The maximum gas temperature for methane combustion is 1850 K. For the validation of the combustion model, the predicted flame temperature for methane combustion is compared to the adiabatic flame temperature. For natural gas or methane fuel and with initial atmospheric conditions (1 bar and $20^0$ C), the theoretical flame temperature produced by the flame with a fast combustion reaction is 1950 K. The predicted maximum temperature of the combustion products or the adiabatic flame temperature compares well with the theoretical adiabatic flame temperature. Fig. 3 shows the profile of temperature along center line. The peak gas temperature is located in the primary reaction zone where the combustion of mixture of air and methane takes place. The fuel from the six injectors is first mixed in the swirling air before burning in the primary reaction zone. The gas temperature decreases after the primary reaction zone due to the dilution of the flame with the secondary air. In this study different equivalence ratio is taken to see the effect of it on temperature and emission level. Fig.6 shows contour of temperature at different equivalence ratio. For lesser equivalence ratio, the maximum achieved temperature is less and flame length is short. As the equivalence ratio increases both maximum temperature and flame length increases significantly. This is due to the fact that increment in equivalence ratio means more mass flow rate of fuel is consumed. Fig.7 shows the variation of temperature at different equivalence ratio (φ). In this profile highest temperature achieved at different location and temperature variation is also different. It is observed that as equivalence ratio increases the variation in temperature increases. Fig.8 shows the variation of NO mass fraction at different equivalence ratio (φ). In this chart we can see that at lowest equivalence ratio φ = 0.27, the value of achieved NO mass fraction is lowest. For equivalence ratio φ=0.33, φ=0.40, φ=0.47, the NO mass fraction increases respectively. The highest value of NO mass fraction is achieved for φ=0.47 because as equivalence ratio increases more fuel is burned in combustion.

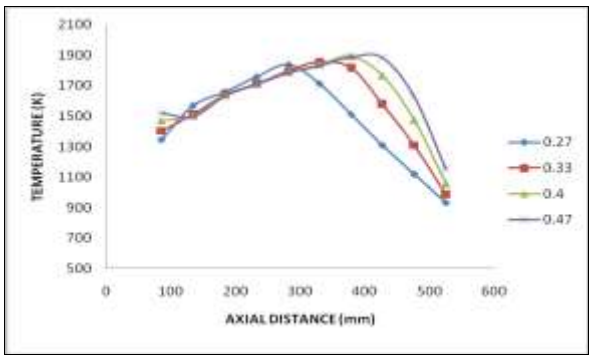


*Fig. 7. Variation of temperature at different equivalence ratio*

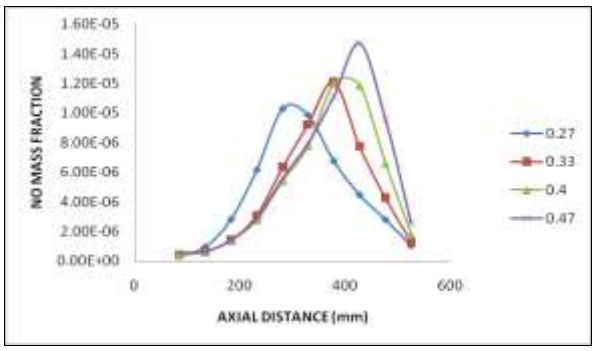


*Fig. 8. Variation of NO mass fraction at different equivalence ratio*

### 3.3. Comparison study of PDF flamelet model and eddy dissipation combustion model

Fig. 9 shows the profile of temperature along center line. In flamelet model maximum temperature achieved at different point than eddy dissipation model.From this we can see eddy dissipation, combustion takes place earlier than the flamelet model.But the initial and exit values are nearly same. Fig. 10 shows the profile of $CO_2$ mass fraction along center line. In flamelet model maximum emission of $CO_2$ achieved at different point than eddy dissipation model. From this we can see the maximum emission of $CO_2$ is more in eddy dissipation.

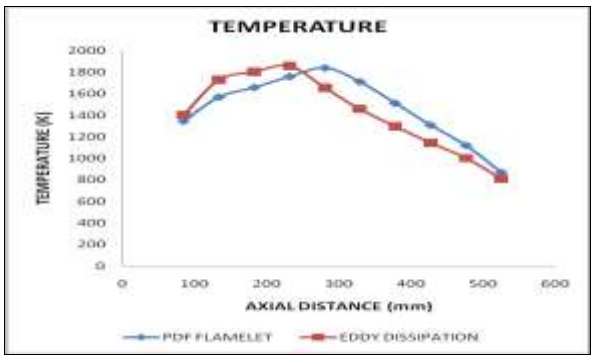


*Fig. 9. Profile of temperature along center line*

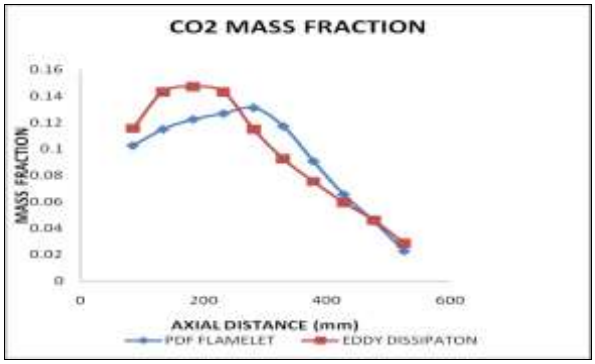


*Fig. 10. Profile of $CO_2$ mass fraction along center line*

Fig. 11 shows the profile of NO mass fractionalong center line. There is more variation in the case of NO mass fraction. From this we can see eddy dissipation, combustion takes place earlier than the flamelet model.

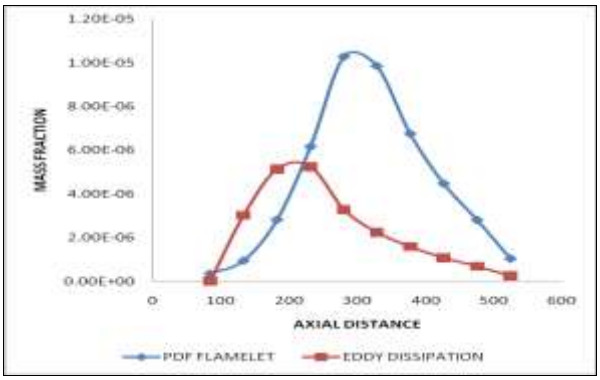


***Fig. 11. Profile of NO mass fraction along center line***

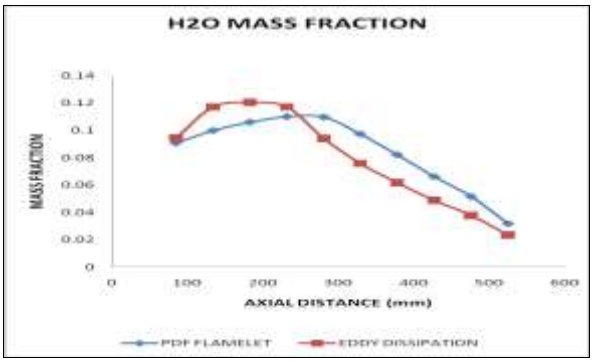


***Fig. 12. Profile of $H_2O$ mass fraction along center line***

Fig. 12 shows the profile of $H_2O$ mass fraction along center line. In flamelet model maximum $H_2O$ mass fraction achieved at different point than eddy dissipation model. Peak value for $H_2O$ mass fraction is in case of eddy dissipation but at outlet the value of mass fraction is more in case of PDF flamelet model. From this we can see eddy dissipation combustion takes place earlier than the flamelet model. Fig. 13 shows the profile of $CH_4$ mass fraction along center line. In flamelet model zero mass

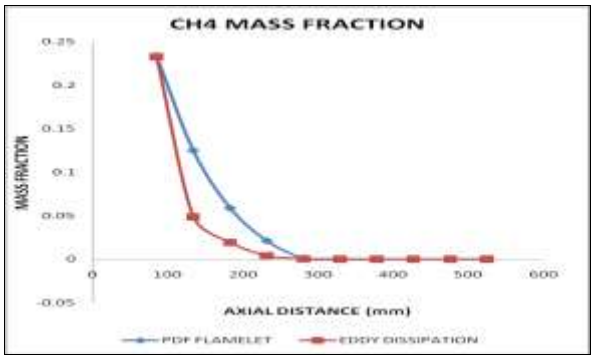


***Fig. 13. Profile of $CH_4$ mass fraction along center line***

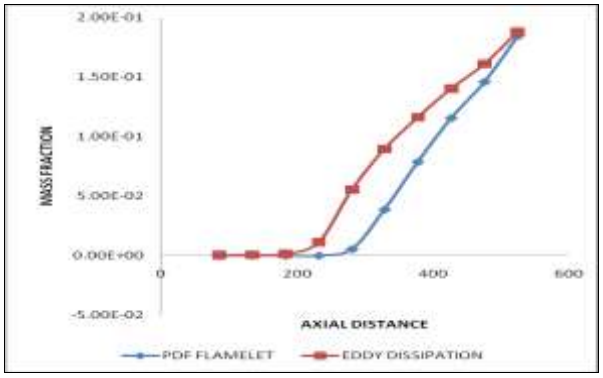


***Fig. 14. Profile of $O_2$ mass fraction along center line***

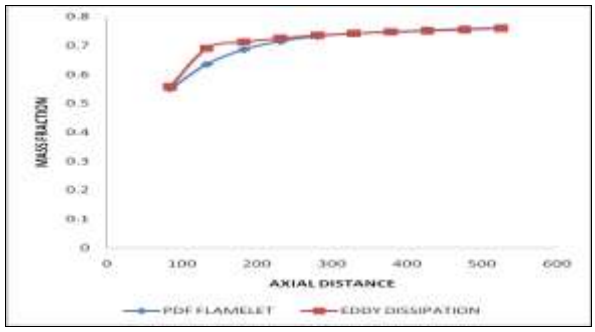


***Fig. 15. Profile of $N_2$ mass fraction along center line***

fraction is achieved at axial distance z =280 mm while in dissipation model this value is achieved at z =230 mm means eddy dissipation combustion takes place earlier than the PDF flamelet model. But the initial and exit values are nearly same Fig. 14 shows the profile of $O_2$ mass fraction along center line. In flamelet model maximum mass fraction achieved at different point than eddy dissipation model. From this we can see eddy dissipation combustion takes place earlier than the flamelet model.But the initial and exit values are nearly same Fig.15 shows the profile of $N_2$ mass fraction along center line. In flamelet model maximum mass fraction achieved at different point than eddy dissipation model.From this we can see eddy dissipation combustion takes place earlier than the flamelet model. But the initial and exit values are nearly same.

## IV. CONCLUSION

The main conclusions from this present study are as follows:

1. 60° swirler geometry is giving less NO emission as the temperature at the exit of combustion chamber is less as compared to 30° and 45° swirler angle geometry. So that for further numerical analysis 60° geometry is used.
2. For methane as fuel and with initial atmospheric conditions, the theoretical flame temperature produced by the flame with a fast combustion reaction is 1950 K. The predicted maximum flame temperature is 1850 K of the combustion products compares well with the theoretical adiabatic flame temperature.
3. Temperature profiles shows increment at reaction zone due to burning of air-methane mixture and decrement in temperature downstream of dilution holes because more and more air will enter in combustion chamber to dilute the combustion mixture along center line . Specie namely NO is increasing and achieving peak point at reaction zone because they are products of combustion along center line.
4. Due to increase in equivalence ratio, temperature and mass fraction of NO increases because more fuel is utilized.
5. From the comparison of Eddy dissipation and PDF flamelet combustion model it is concluded that in Eddy dissipation model combustion takes place earlier than PDF flamelet combustion model.

## REFERENCES

[1] H. Cohen and G.F.C. Rogers, " Gas Turbine Theory", Longman Group Limited, IVth ed. Essex, England
[2] H.A.J.A. van Kuijk , R.J.M. Bastiaans, J.A. van Oijen, L.P.H. de Goey , " Modelling NOx-formation for application in a biomass combustion furnace", Proceedings of the European Combustion Meeting 2005.
[3] Chaouki Ghenai, "Combustion of Syngas Fuel in Gas Turbine Can Combustor", Hindawi Publishing Corporation, Advances in Mechanical Engineering, vol. 2010, 13 pages, Article ID 342357, doi:10.1155/2010/342357.
[4] Tomohiko Furuhata, Shunsuke Amano, Kousaku Yotoriyama, and Masataka Arai, "Development of can-type low NOx combustor for micro gas turbine", J. Fuel, vol. 86, pp 2463 – 2474, 2007.
[5] S Bharat Krishna, and V. Ganesan, "CFD analysis of flow through Vane Swirlers", J. Institution of Engineers, vol. 86, pp 12 – 19, 2005.
[6] Firoj H. Pathan, Nikul K. Patel, and Mihir V. Tadvi, "Combustion of Methane Air Mixture in Gas Turbine Can-Type Combustion Chamber ", International Journal of Scientific and Engineering Research , vol. 3, issue 10, October-2012, ISSN 2229-5518.